

Depletion of *JARID1B* induces cellular senescence in human colorectal cancer

KATSUYA OHTA^{1,2}, NAOTSUGU HARAGUCHI², YOSHIHIRO KANO^{1,2}, YOSHINORI KAGAWA², MASAMITSU KONNO¹, SHIMPEI NISHIKAWA^{1,2}, ATSUSHI HAMABE^{1,2}, SHINICHIRO HASEGAWA^{1,2}, HISATAKA OGAWA^{1,2}, TAKAHITO FUKUSUMI^{1,3}, MAMORU UEMURA², JUNICHI NISHIMURA², TAISHI HATA², ICHIRO TAKEMASA², TSUNEKAZU MIZUSHIMA², YUKO NOGUCHI¹, MIYUKI OZAKI^{1,2}, TOSHIHIRO KUDO¹, DAISUKE SAKAI¹, TAROH SATOH¹, MIWA FUKAMI^{4,5}, MASARU ISHII^{4,5}, HIROFUMI YAMAMOTO², YUICHIRO DOKI², MASAKI MORI² and HIDESHI ISHII¹

Departments of ¹Frontier Science for Cancer and Chemotherapy; ²Gastroenterological Surgery and ³Otorhinolaryngology-Head and Neck Surgery, Osaka University, Graduate School of Medicine; ⁴Laboratory of Cellular Dynamics, WPI-Immunology Frontier Research Center, Osaka University, Suita, Osaka 565-0871; ⁵Japan Science and Technology Agency, Core Research for Evolutional Science and Technology (JST-CREST), Chiyoda-ku, Tokyo 102-0075, Japan

Received September 18, 2012; Accepted November 2, 2012

DOI: 10.3892/ijo.2013.1799

Abstract. The global incidence of colorectal cancer (CRC) is increasing. Although there are emerging epigenetic factors that contribute to the occurrence, development and metastasis of CRC, the biological significance of epigenetic molecular regulation in different subpopulations such as cancer stem cells remains to be elucidated. In this study, we investigated the functional roles of the H3K4 demethylase, *jumonji*, *AT rich interactive domain 1B* (*JARID1B*), an epigenetic factor required for the continuous cell growth of melanomas, in CRC. We found that CD44⁺/aldehyde dehydrogenase (ALDH)⁺ slowly proliferating immature CRC stem cell populations expressed relatively low levels of *JARID1B* and the differentiation marker, CD20, as well as relatively high levels of the tumor suppressor, *p16/INK4A*. Of note, lentiviral-mediated continuous *JARID1B* depletion resulted in the loss of epithelial differentiation and suppressed CRC cell growth, which was associated with the induction of phosphorylation by the c-Jun N-terminal kinase (Jnk/Sapk) and senescence-associated β -galactosidase activity.

Moreover, green fluorescent-labeled cell tracking indicated that *JARID1B*-positive CRC cells had greater tumorigenicity than *JARID1B*-negative CRC cells after their subcutaneous inoculation into immunodeficient mice, although *JARID1B*-negative CRC cells resumed normal growth after a month, suggesting that continuous *JARID1B* inhibition is necessary for tumor eradication. Thus, *JARID1B* plays a role in CRC maintenance. *JARID1B* may be a novel molecular target for therapy-resistant cancer cells by the induction of cellular senescence.

Introduction

Human colorectal cancer (CRC) is one of the most frequently diagnosed cancers in the Western world and a leading cause of mortality in the USA. Genetic events (mutations, deletions, genome amplifications and chromosome translocations) are involved in the initiation and progression of CRC and their stepwise accumulation is a driving force of malignancies (1). Epigenetic regulation also plays a critical role in the pathogenesis of CRC. DNA methylation is a component of the epigenetic gene-silencing complex (2), whereas histone (H3 and H4) post-translational modifications comprise a ubiquitous component of rapid epigenetic changes (3). Epigenetic changes are associated with altered transcription (4). Metastasis correlates with the loss of epithelial differentiation, induction of epithelial mesenchymal transition and the acquisition of a migratory phenotype, which are controlled by epigenetic alterations caused by the dysregulation of the transcriptome in CRC (4).

The basic nucleosome unit has four core histone proteins (H2A, H2B, H3 and H4). Histones H3 and H4 are generally associated with active gene transcription. Their acetylation levels are crucial with respect to the chromatin status and regulation of gene expression (5). Using the H3K4 demethylase, *jumonji*, *AT rich interactive domain 1B* (*JARID1B*), as a biomarker, a small subpopulation of tumor-initiating cells was

Correspondence to: Professor M. Mori, Department of Gastroenterological Surgery, Osaka University, Graduate School of Medicine, 2-2 Yamadaoka, Suita, Osaka 565-0871, Japan
E-mail: mmori@gesurg.med.osaka-u.ac.jp

Professor H. Ishii, Department of Frontier Science for Cancer and Chemotherapy, Osaka University, Graduate School of Medicine, 2-2 Yamadaoka, Suita, Osaka 565-0871, Japan
E-mail: hishii@gesurg.med.osaka-u.ac.jp

Key words: *jumonji*, *AT rich interactive domain 1B*, H3K4 demethylase, epigenome, tumor suppressor genes, cellular senescence, colorectal cancer

isolated from a melanoma sample (6). *JARID1B* depletion has been shown to eliminate melanoma cell growth (6). Therefore, in this study, we investigated the effect of *JARID1B* depletion by lentiviral transfer of small hairpin RNA (shRNA) molecules on CRC cells. We identified a novel phenotype and cellular senescence in CRC induced by continuous *JARID1B* depletion, as well as tumor elimination and regression, which suggests a potential role for *JARID1B* in CRC diagnosis and therapy.

Materials and methods

Immunohistochemistry. Immunohistochemical staining was performed on 4- μ m sections of formalin-fixed, paraffin-embedded surgical tumor samples. The sections were mounted, deparaffinized in xylene and rehydrated in descending concentrations of ethanol. Antigen retrieval was performed using citrate buffer (10 mM, pH 6.0) heated in a pressure cooker for 5 min. The blocking of endogenous peroxidases was accomplished by incubating the sections in 3% hydrogen peroxide (H_2O_2 ; Wako Pure Chemical Industries, Ltd.) for 5 min. The sections were incubated with rabbit anti-JARID1B antibody (1:100; Novus Biologicals) overnight at 4°C. Immunostaining for JARID1B was performed using the Envision + Dual Link System and Vectastain ABC kit (Vector Laboratories) according to the manufacturer's instructions. The sections were counterstained with hematoxylin and eosin.

Cell culture. Three CRC cell lines (Colo201, DLD1 and HCT116) were used. Colo201 and DLD1 cells were cultured in RPMI-1640 supplemented with 10% fetal bovine serum (FBS). HCT116 and human embryonic kidney (HEK)-293T cells were cultured in Dulbecco's modified Eagle's medium (DMEM) supplemented with 10% FBS. Transfection was performed using FuGENE-6 (Roche) transfection reagent according to the manufacturer's instructions, followed by lentiviral production in HEK-293T cells and viral infection (Roche).

Proliferation and MTT assays. Quantification of cell proliferation was based on measurements of bromodeoxyuridine (BrdU) incorporation during DNA synthesis in replicating (cycling) cells using the BrdU Cell Proliferation ELISA kit (colorimetric) (Roche). The cells (1.0×10^5) were incubated with $0.1 \times 10^{-2} \mu$ M 5-fluorouracil (5-FU; Kyowa Hakko Kirin Co., Ltd.) for 48 h and analyzed using the Cell Proliferation kit I (MTT; Roche).

Flow cytometry and cell sorting. Allophycocyanin (APC)-conjugated anti-human CD44 (BD Biosciences) and fluorescein isothiocyanate-conjugated anti-human aldehyde dehydrogenase (ALDH; the Aldefluor kit, Aldagen) were used to characterize cancer cells. Labeled cells (1×10^6) were analyzed using the BD FACSAria II cell sorter system (Becton-Dickinson), followed by data analysis using the Diva program (Becton-Dickinson). The fluorescent ubiquitination-based cell cycle indicator (Fucci)-G1 DsRed2 contains a fragment of human Cdt1 (amino acids 30-120), which is ubiquitinated by the ubiquitin ligase complex SCF^{skp2} during the S and G2 phases and degraded by proteasomes, thereby denoting the G1 phase (7). Fucci-S/G2/M Green contains a fragment of human geminin (amino acids 1-110)

linked to enhanced green fluorescent protein (EGFP), which is ubiquitinated by the E3 ligase complex APC^{cdh1} and degraded by proteasomes during the M and G1 phases, denoting the S, G2 and M phases (7). DsRed2 and mKO2 or EGFP and mAG were excited by 488-nm laser lines and their emission was detected with 530/30BP and 585/42BP filters, respectively.

Reactive oxygen species (ROS) assay and senescence-associated (SA) β -galactosidase (SA- β -gal) analysis. The ROS assay was performed as described previously (8). To evaluate the effects of ROS, 10 μ M N-acetyl cysteine (NAC; Wako Pure Chemical Industries, Ltd.), a general antioxidant and ROS inhibitor, was added. The cells (2×10^5) were treated with 20-100 μ M H_2O_2 (Wako Pure Chemical Industries, Ltd.) for 1 h to induce oxidative stress. Intracellular ROS and SA- β -gal (the Senescence Detection kit) were analyzed using NAC (9). Intracellular ROS levels were determined by incubating the cells for 30 min at 37°C with 5 μ M CellROX™ Deep Red reagent (Invitrogen Life Technologies) in complete medium, followed by cytometry.

Protein analysis. Western blot analysis and immunoprecipitation were performed. Total cell lysates were prepared using lysis buffer [50 mM 4-(2-hydroxyethyl)-1-piperazineethanesulfonic acid (HEPES) (pH 7.5), 150 mM NaCl, 1% TritonX-100] containing ethylenediaminetetraacetic acid (EDTA)-free protease inhibitors. Cell lysates containing 20 μ g of protein were electrophoresed on TGX™ gels (Bio-Rad). Subsequently, proteins were transferred onto a PVDF membrane (Bio-Rad). The primary antibodies were JARID1B (1:2,000; Novus Biologicals), c-Jun N-terminal kinase (Jnk/Sapk; 1:1,000; Cell Signaling Technology, Danvers, MA), phospho-Jnk/Sapk (1:1,000; Cell Signaling Technology) and β -actin (loading control; 1:5,000; Cell Signaling Technology). Western blotting signals were detected and quantified by image analysis software (Multi Gauge version 3, Fujifilm). The means \pm standard deviation (SD) of three independent experiments were determined.

Chromatin immunoprecipitation (ChIP) analysis. ChIP analysis was performed using the ChIP-IT Express Enzymatic kit (Active Motif, Carlsbad, CA). The antibodies used for ChIP analysis were histone H3 (ab1791, Abcam), H3K4 me3 (ab8580, Abcam), H3K4 me2 (ab32356, Abcam) and H3K4 me1 (ab8895, Abcam), with rabbit immunoglobulin G (IgG) (ab46540, Abcam) used as the negative control. Immunoprecipitated DNA (100 ng) was quantified by real-time quantitative PCR (qPCR) using the following primers: human *p16/INK4A* promoter, 5'-AACCGCTGCACGCCTCTGAC-3' (forward) and 5'-CCGCGGCTGTCTGAAGGTT-3' (reverse). The means \pm SD of three independent experiments were determined.

RNA interference (RNAi). RNAi involved the transfection of small interfering RNA (siRNA) oligos (Cosmo Bio Co., Ltd) or infection with an shRNA-encoding lentivirus against JARID1B (NM_006618, Sigma-Aldrich) and a control (SHC002, Sigma-Aldrich). The target sequences were as follows: *KDM5B* #1 (100 μ M), GAGCCAGAGCCAUG AAUAUT (sense) and AAUAUCAUGGCCUCUGCUC (anti-

sense), and *KDM5B* #2 (100 μ M), GGAACGAGUUAAGAAAAU (sense) and AUUUUUCUUAACUAGUCCCC (antisense). siRNA oligos were previously validated. siRNA duplexes were transfected into subconfluent cells using Lipofectamine RNAiMAX (Invitrogen Life Technologies). The shRNA target sequence was as follows: *JARID1B*, 5'-CCGGCCACCAATTTGGAAGGCATTCTCGAGAATGCCTTCCAAATTGGTGGGTTTTT-3'.

Real-time reverse transcription PCR (qRT-PCR). Real-time qRT-PCR was performed using a Light Cycler (Roche). Amplified signals were confirmed on the basis of the dissociation curves and normalized against glyceraldehyde-3-phosphate dehydrogenase (*GAPDH*). PCR primer sequences were as follows: human *GAPDH*, 5'-ATGTTTCGTCATGGGTGTGAA-3' (forward) and 5'-TGAGTCCTTCCACGATACCA-3' (reverse); human *JARID1B*, 5'-CGACAAAGCCAAGAGTCTCC-3' (forward) and 5'-GGATAGATCGGCCTCGTGTA-3' (reverse); and human *p16/INK4A*, 5'-GTGTGCATGACGTGGGG-3' (forward) and 5'-GCAGTTCGAATCTGCACCGTAG-3' (reverse). The means \pm SD of three independent experiments were determined.

Animal experiments. Six-week-old female NOD/SCID mice were maintained in a pathogen-free environment. All procedures for animal studies were approved by the Institutional Ethical Committee of the Faculty of Medicine, Osaka University. 1×10^6 tumor cells (viability >90%) per 50 μ l Matrigel (BD Biosciences) were injected subcutaneously. Tumor volume was measured by callipering the largest diameter (A) and its perpendicular (B), and calculated according to the NCI protocol [$TV = (A \times B^2)/2$].

Statistical analysis. Categorical variables were compared by the Chi-square test. Continuous variables (medians/interquartile ranges) were compared using the Wilcoxon test. Statistical analyses were performed using JMP software (JMP version 8.01, SAS Institute). P-values <0.05 were considered to indicate statistically significant differences.

Results

Ubiquitous *JARID1B* expression in clinical samples and various CRC cell lines. A number of studies have revealed the importance of the correlation between different types of cancer (melanoma, prostate and breast cancer) and epigenetic factors; however, to date, no study has suggested the existence of such a correlation for gastrointestinal cancer (6,10,11). *JARID1B* was ubiquitously expressed in some clinical samples of gastrointestinal cancer (modified differentiated adenocarcinoma, Fig. 1A). In addition, we also confirmed ubiquitous *JARID1B* expression in 11 CRC cell lines. Relative *JARID1B* expression in 11 colon adenocarcinoma cell lines and one melanoma cell line (SK MEL) as a positive control was assessed using qPCR (Fig. 1B) (6). Colo201 and HCT116 cells expressed higher *JARID1B* levels than DLD1 cells *in vitro* (Fig. 1C). In the Colo201 and HCT116 cells, the expression of the tumor suppressor, *p16/INK4A*, was increased in *JARID1B*-depleted cells compared with that in the control cells (Fig. 1D), suggesting that *JARID1B* and *p16/INK4A* expression is inversely correlated.

***JARID1B* controls *p16/INK4A* expression.** *JARID1B* plays a role in the compaction of active chromatin, which impedes the access of transcription factors to genes and induces gene silencing (5). Thus, *JARID1B* expression may be associated with cell cycle progression. Fucci transfectants of CRC cells revealed that endogenous *JARID1B* expression increased in the late G1 phase (Fig. 2A and B), suggesting the association of *JARID1B* with *p16/INK4A*, which plays a critical role in the G1-S transition checkpoint (12,13). ChIP analysis indicated that compared with the control cells, multimethylated forms of H3K4 were preferentially associated with the promoter sequence of the *p16/INK4A* genes in *JARID1B*-depleted cells (Fig. 2C). *JARID1B* depletion led to the trimethylation of the *p16/INK4A* promoter (Fig. 2D). Thus, *JARID1B* may play a role in active chromatin compaction of the *p16/INK4A* promoter, which contributes to gene silencing. Therefore, *JARID1B* depletion may lead to *p16/INK4A* activation.

***JARID1B* depletion induces cellular senescence in CRC cells.** *p16/INK4A* is associated with the SA phenotype, which occurs by the retinoblastoma-inhibiting action of cyclin-dependant kinases, leading to G1 cell cycle arrest (13-15), with the involvement of ROS (16). SA- β -gal activity was detected in the *JARID1B*-depleted CRC cells but not in the mock-transfected control cells (Fig. 3A and B). The effect of *JARID1B* depletion on SA- β -gal activity was similar to that of H₂O₂ exposure with an ROS inducer in the medium but not similar to that of the negative experimental control with NAC in the medium (Fig. 3A and B). This suggests that intracellular ROS may be involved in cellular senescence induction. The results from the present study illustrated that intracellular ROS levels were higher in *JARID1B*-depleted CRC cells than in mock-transfected control cells (Fig. 3C), which supports the involvement of ROS in senescence induction in *JARID1B*-depleted cells. Immunoblot analysis of SA phenotypes revealed the increased phosphorylation of Jnk/Sapk, an inducer of cellular senescence, in *JARID1B*-depleted cells; *JARID1B* expression was decreased by RNAi (Fig. 3D).

***JARID1B* depletion suppresses CRC growth.** *JARID1B* depletion suppressed CRC cell growth *in vitro* by intracellular ROS accumulation and cellular senescence activation. Therefore, we investigated its effects on tumor growth *in vivo*. *JARID1B*-positive and -negative CRC cells were sorted using a fluorescent tracer vector controlled by the *JARID1B* promoter (Fig. 4A). CRC cells were separated on the basis of d2-Venus expression and the fluorescent intensity depended on the endogenous expression of the *JARID1B* promoter (Fig. 4B). *JARID1B*-positive and -negative CRC cells were subcutaneously inoculated into immunodeficient NOD/SCID mice to assess their tumorigenicity (Fig. 4C). Endogenous *JARID1B*-positive CRC cells produced substantial tumor growth compared with the *JARID1B*-negative cells (Fig. 4D).

***JARID1B* depletion suppresses therapy-resistant CRC cell growth.** We measured cell proliferation following *JARID1B* depletion and observed that *JARID1B* depletion significantly suppressed cell proliferation (Fig. 5A) and cell invasion (data not shown). Hence, we determined the resistance of CRC cells to chemotherapy, a feature of *JARID1B*-depleted cells (17,18).

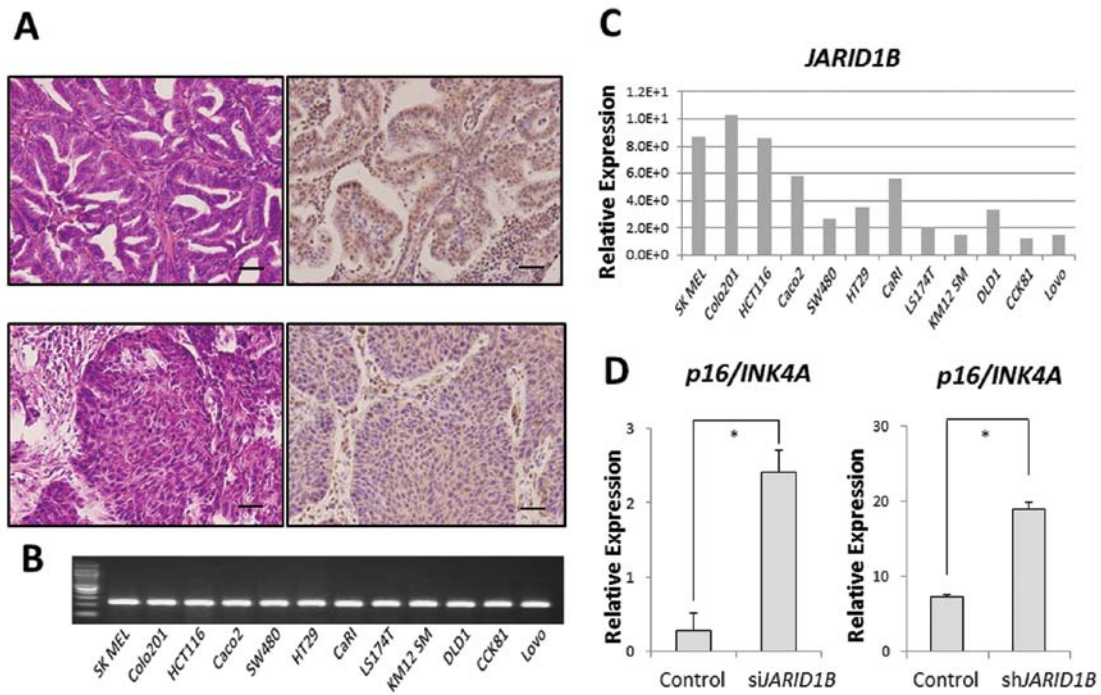


Figure 1. Ubiquitous *JARID1B* expression in clinical samples and cell lines. (A) A sample of clinical colon adenocarcinoma (moderately differentiated); left panel, hematoxylin and eosin staining (x200); right panel, immunohistological staining of *JARID1B* (x200). Scale bar, 100 μ m. (B) *JARID1B* expression in 11 CRC cell lines and one positive control (SK MEL). (C) Relative *JARID1B* expression in 11 CRC cell lines and one positive control (SK MEL). (D) Both synthesized oligo RNA-mediated (siRNA) and lentiviral-mediated depletion (shRNA) of endogenous *JARID1B* resulted in a significant increase in *p16/INK4A* expression in Colo201 cells. Relative expression is shown.

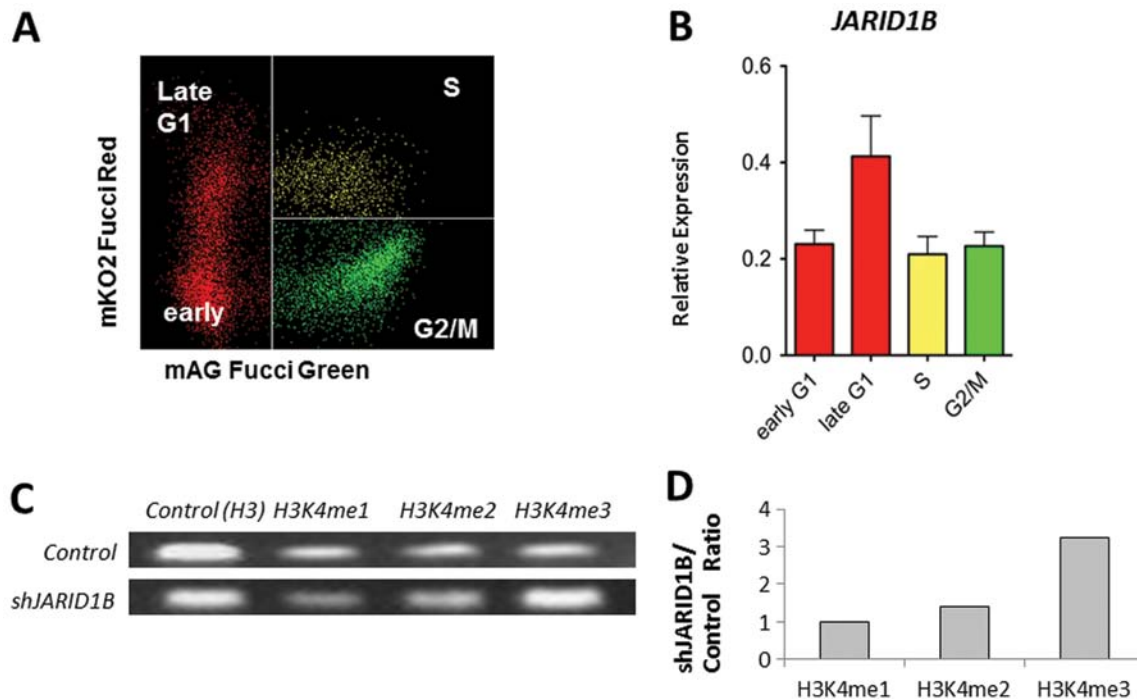


Figure 2. *JARID1B* controlled cell cycle and *p16/INK4A* expression. (A) Cell cycle phase of Fucci-labeled HCT116 cells separated by flow cytometry and FACS. (B) Relative *JARID1B* expression by stage (early and late G1, S and G2/M). (C) ChIP assay of the promoter region of *p16/INK4A* in Colo201 cells. (D) The relative ratio is shown in columns. me1, monomethyl; me2, dimethyl; me3, trimethyl. The control includes all methyl modifications.

The MTT assay illustrated that compared with the controls, continuous *JARID1B* depletion induced resistance to 5-FU in culture (Fig. 5B), suggesting that *JARID1B* depletion contrib-

utes to cancer stem cell (CSC) suppression. The depletion of endogenous *JARID1B* has been shown to suppress tumorigenicity and eliminate CSCs in melanomas (6). Thus, we

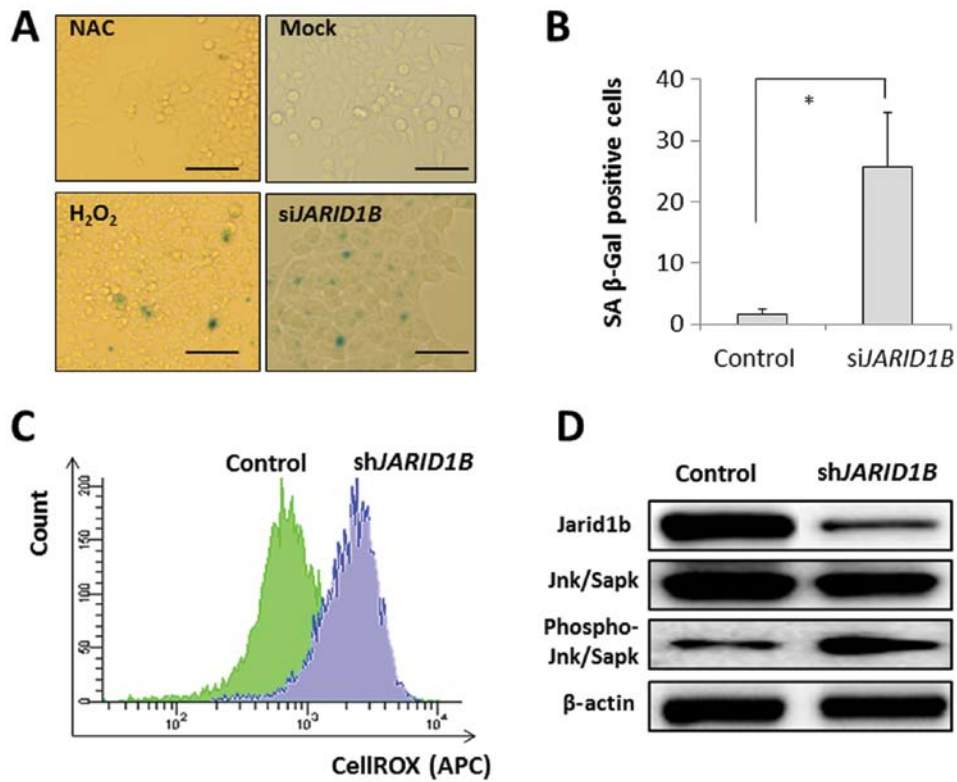


Figure 3. Induction of CRC cellular senescence by *JARID1B* depletion. (A) Phase-contrast microscopy of SA-β-gal activity in *JARID1B*-depleted and control Colo201 cells. NAC, N-acetyl cysteine; H₂O₂, hydrogen peroxide. Scale bar, 100 μm. (B) Quantitative analysis of SA-β-galactosidase in Colo201 cells. (C) Intracellular ROS levels measured using CellROX-labeled APC and flow cytometry in Colo201 cells. (D) Immunoblot analysis of SA proteins in *JARID1B*-depleted and control Colo201 cells.

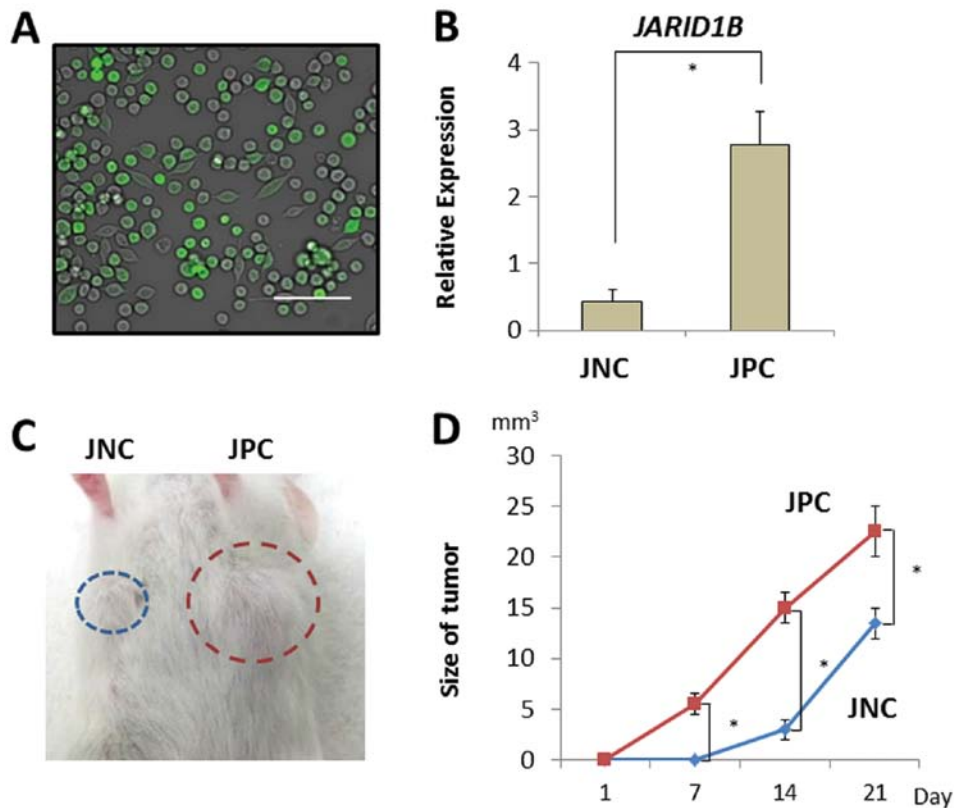


Figure 4. Tumorigenicity of *JARID1B*-depleted cells. (A) Visualization of *JARID1B* promoter activity using fluorescent d2-Venus labeling. (B) Quantitative RT-PCR analysis of *JARID1B* in sorted endogenous *JARID1B*-expressing and *JARID1B*-non-expressing CRC Colo201 cells (JPCs and JNCs, respectively). (C) Three weeks after injection, JPCs (blue circle) and JNCs (red circle) in mice. (D) Tumorigenicity of sorted endogenous JPCs or JNCs. JPCs had higher tumorigenicity.

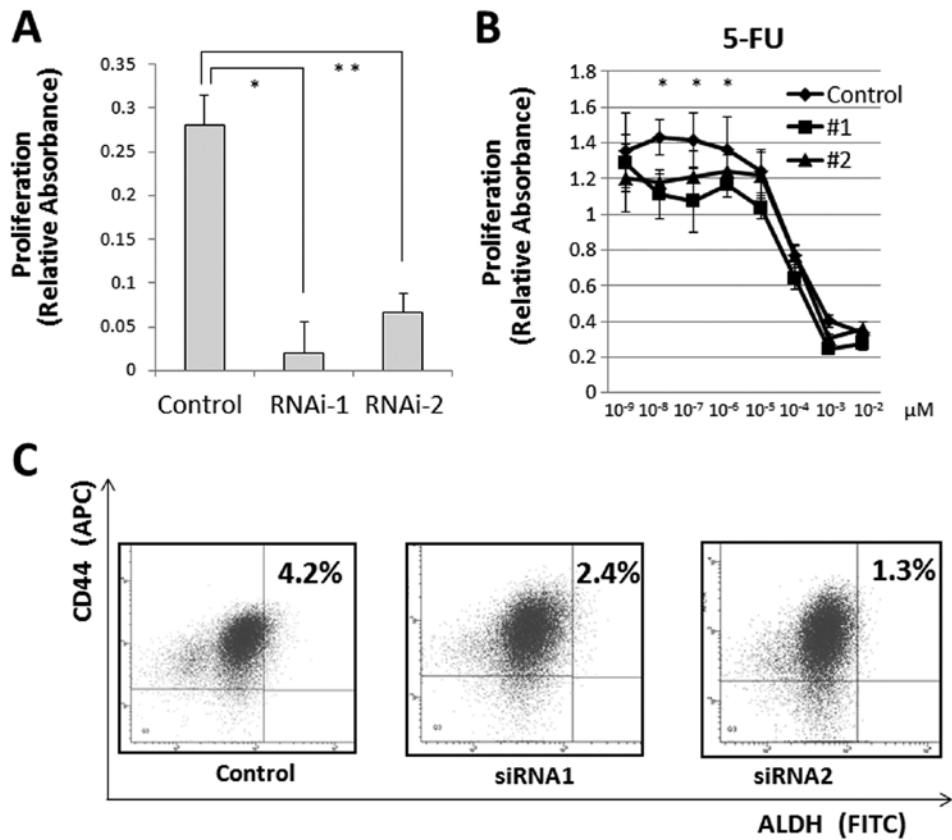


Figure 5. Suppression of cell growth and chemoresistance by *JARID1B* depletion. (A) Lentiviral-mediated depletion of endogenous *JARID1B* suppressed Colo201 cell proliferation compared with that of the controls, as shown by MTT assay (proliferation assay). (B) Chemoresistance assay. *JARID1B*-depleted and control Colo201 cells were exposed to 5-FU in an MTT assay (proliferation assay). (C) Flow cytometric analyses of endogenous *JARID1B*-depleted Colo201 cells (#1 and #2). CD44⁺/ALDH⁺ fractions were smaller in *JARID1B*-depleted cells than in the control cells.

inhibited endogenous *JARID1B* using shRNA and confirmed the CSC fraction. Depletion of endogenous *JARID1B* reduced the CD44⁺/ALDH⁺ CSC fraction, indicating that continuous endogenous *JARID1B* inhibition contributed to the eradication of CRC stem cells (Fig. 5C).

Discussion

Histone methylation/demethylation generally deactivates and activates genes by controlling the access of transcription factors to DNA. Histone dysregulation caused by genetic and epigenetic alterations is a hallmark of cancer (9,19). *JARID1A/B*-mediated histone H3K4 demethylation contributes to the silencing of retinoblastoma target genes in senescent cells, presumably by compacting chromatin and silencing certain genes (20). Distinct SA changes in histone-modification patterns are consistent with a repressive chromatin environment in the retinoblastoma tumor suppressor pathway (20). We found that *JARID1B* depletion, i.e., the inhibition of H3K4 demethylation, stimulated *p16/INK4A* transcription and suppressed tumor cell growth *in vitro* and *in vivo*, suggesting that it plays a role in cell growth regulation in human CRC (6).

The present findings are consistent with the notions that *JARID1B* depletion induces Jnk/Sapk-related senescence in CRC cells (21) and that endogenous *JARID1B* plays a role in controlling the cellular growth of CRCs. In cellular senescence, normal diploid cells lose the ability to divide. This

anti-proliferative stress-response program acts as a potent tumor-suppressing mechanism (14,22). Growth-promoting and tumor suppressor genes are important factors controlling cancer cell proliferation. Cellular senescence can be triggered by a number of factors, including aging, DNA damage, oncogene activation and oxidative stress. Senescent cells have distinctive features, including stable cell cycle arrest and SA- β -gal activity. The tumor suppressor *p16/INK4A* plays a key role in regulating senescence induction, as may the tumor suppressor, p53. p16 acts through the retinoblastoma pathway to inhibit cyclin-dependant kinases, leading to G1 cell cycle arrest and senescence (14,23). Our results demonstrate that *JARID1B* plays a key role in CRC maintenance and that its continuous inhibition induces cellular senescence.

In the present study, we present a novel hypothesis that *JARID1B* suppression is an essential factor in cancer eradication. Although CSCs play a critical role in the survival, relapse and metastasis of malignant cancer cells (17), our data confirm the correlation between *JARID1B* suppression and CSCs. ALDH and CD44, a hyaluronic acid receptor, are considered useful markers of CRC stem cells (18). ALDH1A1 is responsible for CSC ALDH activity (24). It is known that CD44⁺/ALDH⁺ double-positive cells are CSC enrichment markers for reconstituted tumors in immunodeficient mice (18,24). In our study, endogenous *JARID1B* expression was lower in CD44⁺/ALDH⁺ cells than in CD44⁺/ALDH⁻ or CD44⁻/ALDH⁻ cells, suggesting that slowly proliferating *JARID1B*-expressing

cells had a relatively undifferentiated phenotype that was compatible with that of CSCs (17,18). Our results demonstrate that *JARID1B* is involved in cell cycle regulation and that *JARID1B* facilitates cellular amplification and CSC maintenance. Future reports should further clarify the correlation between epigenetic factors and CSCs.

Therapeutic approaches to CRC include conventional therapies (surgical removal and chemoradiotherapy) and gene delivery strategies. For example, continuous *JARID1B* depletion could be achieved with antisense oligonucleotides or low-molecular-weight pharmacological therapeutics (25). A combination of *p16/INK4A* gene therapy and anti-*JARID1B* treatment may lead to the efficient induction of a SA phenotype in CRC cells.

Acknowledgements

We thank Dr Atsushi Miyawaki for providing us with the Fucci System plasmids. This study was partly supported by a Grant-in-Aid for Scientific Research from the Ministry of Education, Culture, Sports, Science and Technology (H.I. and M.M.); a Grant-in-Aid from the 3rd Comprehensive 10-year Strategy for Cancer Control, Ministry of Health, Labour and Welfare (H.I. and M.M.); a grant from the Kobayashi Cancer Research Foundation (H.I.); and a grant from the Princess Takamatsu Cancer Research Fund, Japan (H.I.). M.K., T.K., D.S., T.S. and H.I. were partially supported by Chugai Co., Ltd. and Yakult Honsha Co., Ltd. via institutional endowments.

References

1. Markowitz SD and Bertagnolli MM: Molecular origins of cancer: Molecular basis of colorectal cancer. *N Engl J Med* 361: 2449-2460, 2009.
2. Patai AV, Molnár B, Kalmár A, Schöller A, Tóth K and Tulassay Z: Role of DNA methylation in colorectal carcinogenesis. *Dig Dis* 30: 310-315, 2012.
3. Gargalionis AN, Piperi C, Adamopoulos C and Papavassiliou AG: Histone modifications as a pathogenic mechanism of colorectal tumorigenesis. *Int J Biochem Cell Biol* 44: 1276-1289, 2012.
4. Brabletz T, Jung A, Spaderna S, Hlubek F and Kirchner T: Opinion: migrating cancer stem cells-an integrated concept of malignant tumour progression. *Nat Rev Cancer* 5: 744-749, 2005.
5. Kouzarides T: Chromatin modifications and their function. *Cell* 128: 693-705, 2007.
6. Roesch A, Fukunaga-Kalabis M, Schmidt EC, *et al*: A temporarily distinct subpopulation of slow-cycling melanoma cells is required for continuous tumor growth. *Cell* 141: 583-594, 2010.
7. Sakaue-Sawano A, Kurokawa H, Morimura T, *et al*: Visualizing spatiotemporal dynamics of multicellular cell-cycle progression. *Cell* 132: 487-498, 2008.
8. Haraguchi N, Ishii H, Mimori K, *et al*: CD13 is a therapeutic target in human liver cancer stem cells. *J Clin Invest* 120: 3326-3339, 2010.
9. Takahashi A, Imai Y, Yamakoshi K, *et al*: DNA damage signaling triggers degradation of histone methyltransferases through APC/C(Cdh1) in senescent cells. *Mol Cell* 45: 123-131, 2012.
10. Yamane K, Tateishi K, Klose RJ, *et al*: PLU-1 is an H3K4 demethylase involved in transcriptional repression and breast cancer cell proliferation. *Mol Cell* 25: 801-812, 2007.
11. Xiang Y, Zhu Z, Han G, *et al*: *JARID1B* is a histone H3 lysine 4 demethylase up-regulated in prostate cancer. *Proc Natl Acad Sci USA* 104: 19226-19231, 2007.
12. Kastan MB and Bartek J: Cell-cycle checkpoints and cancer. *Nature* 432: 316-323, 2004.
13. Ohtani N, Zebedee Z, Huot TJ, *et al*: Opposing effects of Ets and Id proteins on p16INK4a expression during cellular senescence. *Nature* 409: 1067-1070, 2001.
14. Rayess H, Wang MB and Srivatsan ES: Cellular senescence and tumor suppressor gene p16. *Int J Cancer* 130: 1715-1725, 2012.
15. Zhang X, Wu X, Tang W and Luo Y: Loss of p16(Ink4a) function rescues cellular senescence induced by telomere dysfunction. *Int J Mol Sci* 13: 5866-5877, 2012.
16. Vurusaner B, Poli G and Basaga H: Tumor suppressor genes and ROS: complex networks of interactions. *Free Radic Biol Med* 52: 7-18, 2012.
17. Reya T, Morrison SJ, Clarke MF and Weissman IL: Stem cells, cancer and cancer stem cells. *Nature* 414: 105-111, 2001.
18. Dewi DL, Ishii H, Kano Y, *et al*: Cancer stem cell theory in gastrointestinal malignancies: recent progress and upcoming challenges. *J Gastroenterol* 46: 1145-1157, 2011.
19. Hanahan D and Weinberg RA: Hallmarks of cancer: the next generation. *Cell* 144: 646-674, 2011.
20. Chicas A, Kapoor A, Wang X, *et al*: H3K4 demethylation by *Jarid1a* and *Jarid1b* contributes to retinoblastoma-mediated gene silencing during cellular senescence. *Proc Natl Acad Sci USA* 109: 8971-8976, 2012.
21. Maruyama J, Naguro I, Takeda K and Ichijo H: Stress-activated MAP kinase cascades in cellular senescence. *Curr Med Chem* 16: 1229-1235, 2009.
22. Rodier F and Campisi J: Four faces of cellular senescence. *J Cell Biol* 192: 547-556, 2011.
23. Ohtani N, Mann DJ and Hara E: Cellular senescence: its role in tumor suppression and aging. *Cancer Sci* 100: 792-797, 2009.
24. Marcato P, Dean CA, Giacomantonio CA and Lee PW: Aldehyde dehydrogenase: its role as a cancer stem cell marker comes down to the specific isoform. *Cell Cycle* 10: 1378-1384, 2011.
25. Yamamoto T, Nakatani M, Narukawa K and Obika S: Antisense drug discovery and development. *Future Med Chem* 3: 339-365, 2011.